The Journal of Veterinary Medical Science

NOTE

Internal Medicine

Intrapancreatic accessory spleen mimicking pancreatic insulinoma with intrapancreatic metastasis in a cat

Shintaro TOMURA[1)], Atsushi TOSHIMA[1)], Akira NOMURA[1)], Masahiko HIRATA[2)], Tetsushi YAMAGAMI[3)], Yumiko KAGAWA[3)] and Tsuyoshi KADOSAWA[1)]*

[1)]Japan Small Animal Medical Center, Saitama, Japan
[2)]IDEXX Laboratories, KK, Tokyo, Japan
[3)]North Lab, Hokkaido, Japan

J. Vet. Med. Sci.
84(3): 439–444, 2022
doi: 10.1292/jvms.21-0584

Received: 30 October 2021
Accepted: 24 January 2022
Advanced Epub:
2 February 2022

ABSTRACT. An 11-year-old neutered male Domestic Shorthair cat presented with a 3-month history of hypoglycemia, two episodes of seizure, and intermittent tick-like signs. Serum biochemistry revealed severe hypoglycemia associated with high insulin concentrations. Dynamic abdominal computed tomography (CT) indicated two pancreatic masses, which were enhanced most during the late arterial phase but had different degrees and variations of attenuation. Partial pancreatectomy was performed. Histopathology and immunohistochemistry confirmed that one mass was an insulinoma and the other was an ectopic splenic tissue, consistent with the differences in imaging findings. When an intrapancreatic lesion with hyper-attenuation on dynamic abdominal CT is detected, not only insulinoma or metastasis of malignancies but also intrapancreatic accessory spleen (IPAS) should be considered as differential diagnoses.

KEY WORDS: arterial phase, dynamic computed tomography, insulinoma, intrapancreatic accessory spleen

Pancreatic insulinomas are functional beta cell tumors that cause persistent hypoglycemia because of inappropriate insulin secretion. Although there are various reports of canine pancreatic insulinomas [3, 17, 21, 23], the tumors are extremely rare in cats, with only nine well-documented cases in the literature [4, 11–13, 16, 25, 27, 33, 34]. Diagnostic imaging modalities for canine pancreatic insulinomas reported previously include ultrasonography [20, 28, 31, 37], contrast-enhanced ultrasonography [26, 39], computed tomography (CT) [2, 6, 8, 14, 24, 31], single-photon emission CT (SPECT) [31, 32] and somatostatin receptor scintigraphy [10, 22]. CT is more sensitive than ultrasonography and single-photon CT for the detection of pancreatic insulinomas in dogs [31]. However, of the previous nine feline cases, only one involved CT confirmation of a pancreatic mass before surgery [34].

Ectopic spleen is defined as histopathologically normal splenic tissues in an abnormal location, and it can be classified as accessory spleen or splenosis [1, 30]. While accessory spleen is a congenital condition, splenosis is a secondary lesion associated with splenic rupture or splenectomy [1, 7, 18, 30]. In cats, cases of ectopic spleen associated with the omentum and pancreas have been reported, but no imaging findings have been noted [29, 35, 38].

Herein, we report a cat case in which dynamic abdominal CT showed two pancreatic lesions suspected to be pancreatic insulinomas. Since both surgically removed lesions were diagnosed histopathologically as an insulinoma and ectopic splenic tissue, we focus on the imaging findings of both lesions.

An 11-year-old neutered male Domestic Shorthair cat weighing 6.9 kg was presented to the Japan Small Animal Medical Center with a 3-month history of hypoglycemia, two episodes of seizures, and intermittent tick-like signs. Before referral, the patient was administered a concentrated glucose solution orally twice per day. However, the neurological signs did not completely disappear. On presentation, the patient was bright and alert. Physical and neurological examinations revealed no abnormalities. Informed consent for all procedures was provided by the owners.

The results of the complete blood cell count (Procyte DX; IDEXX, Tokyo, Japan) were within reference intervals (RI). Serum biochemical abnormalities (FUJI DRI-CHEM 7000V; FUJIFILM, Tokyo, Japan) included hypoglycemia (32 mg/dl; RI, 71–148 mg/dl) and hyperammonemia (213 µg/dl; RI, 23–78 µg/dl). Concurrently, the insulin concentration (FUJIFILM VET Systems, Tokyo, Japan) increased (61.6 µU/ml; RI, 7.0–17.9 µU/ml). Urinalysis revealed a urine specific gravity of 1.022.

*Correspondence to: Kadosawa, T.: kadosawa@jsamc.jp, Japan Small Animal Medical Center, 1-10-4 Higashi-tokorozawa, Tokorozawa, Saitama 359-0025, Japan

Thoracic and abdominal radiographs were unremarkable. Abdominal ultrasonography (ARIETTA 70; HITACHI, Tokyo, Japan) revealed an oval isoechoic mass measuring up to 18 mm in length in the apex of the right pancreatic lobe region (Fig. 1). However, it could not be determined whether the mass originated from the pancreas.

Dynamic abdominal CT (Aquilion PRIME; TOSHIBA, Tokyo, Japan) was performed under general anesthesia. At our facility, a four-phase series was obtained for every dynamic abdominal CT scan for pancreatic diseases using the bolus-tracking technique. After the pre-contrast scan, a non-ionic iodinated contrast medium, iopamidol (Oypalomin; Fuji Pharma, Tokyo, Japan), was injected via the cephalic vein at a dose of 750 mg iodine/kg with a 15-sec injection duration using an angiographic power injector. The first scan was started immediately after the CT value of the aorta at the level of the cranial side of the liver had reached 150 Hounsfield units (HU). The second scan was started 3 sec after the first scan was completed. The third and fourth scans were started 50 sec and 120 sec after starting the injection, respectively. The second scan was performed in the caudocranial direction; however, the other three scans were performed in the craniocaudal direction. The phases were early arterial phase, late arterial phase, portal vein phase, and equilibrium phase. The standard algorithm was used and the scan and reconstruction parameters were as follows: tube voltage, 120 kVp; tube current, 350 mA; slice thickness, 0.5 mm; rotation time, 0.5 sec; beam pitch, 0.813; and reconstruction interval, 0.5 mm.

The acquired CT images were reviewed using image processing software (OsiriX; Pixmeo, Geneva, Switzerland) and revealed two pancreatic lesions. One was an 18-mm mass originating from the apex of the right pancreatic lobe and the other was a 4-mm nodule in the distal part of the left pancreatic lobe. Both lesions were similarly enhanced most during the late arterial phase. A single anomalous vessel was confirmed to anastomose the splenic vein with the left phrenic vein. There were no enlarged or enhanced lymph nodes or nodules in the liver. No abnormalities were observed using head magnetic resonance imaging (MRI) (AIRIS Vento; HITACHI) and cerebrospinal fluid.

Ultrasound-guided fine-needle aspiration was performed; however, samples were obtained only from the right lobe mass because the nodule was not delineated from the left lobe parenchyma. Cytological examination revealed clusters of epithelial cells with light basophilic cytoplasm and oval nuclei containing fine reticular chromatin (Fig. 1).

Based on these findings, a clinical diagnosis of hypoglycemia as a paraneoplastic syndrome of pancreatic insulinoma with intrapancreatic metastasis that may have caused several neurological signs was proposed. To resolve hypoglycemia and make a definitive diagnosis, surgical excision of the right lobe mass and left lobe nodule was suggested and agreed upon by the owner.

Surgery was performed 16 days after the referral. A solitary reddish mass was identified at the apex of the right lobe (Fig. 2), and a blood blister-like nodule was found distal to the left lobe (Fig. 3). Partial pancreatectomy of the right and left lobes was performed using a vessel sealing system and hemoclips. Liver biopsy samples were obtained from the left lateral lobe and the right internal lobe. The remaining abdominal cavity and organs were macroscopically normal. All samples were subjected to histopathological and immunohistochemical analyses.

Hypoglycemia was resolved immediately after surgery (197 mg/dl) and the insulin concentration decreased (10.9 µU/ml) on the day after surgery. At a year after surgery, the patient was clinically normal and had a normal serum glucose concentration (118 mg/dl). Based on the clinical course, hypoglycemia was definitively diagnosed as a paraneoplastic syndrome of pancreatic insulinoma that caused several neurological signs.

The right lobe mass was histopathologically determined to be an islet cell tumor (Fig. 2), and the left lobe nodule was determined to be an ectopic splenic tissue (Fig. 3). Additionally, immunohistochemical staining was performed using human insulin antibody (K36aC10; Nichirei, Tokyo, Japan). Peroxidase activity was demonstrated using diaminobenzidine solution, and the sample slides were counterstained with hematoxylin. The diagnosis of an insulinoma was confirmed as the tumor cells were diffusely positive for insulin (Fig. 2). The tumor was well-circumscribed, and there were no tumor cells in the margins. Insulinoma cells were not observed upon examination of the submitted liver biopsy samples.

Based on unpredictable histopathological diagnoses, we reevaluated the CT value changes on dynamic abdominal CT of the two pancreatic lesions, which were insulinoma and ectopic splenic tissue, and compared them to those of the normal surrounding pancreatic parenchyma and the normal splenic parenchyma. The CT values of the normal splenic parenchyma were measured at the

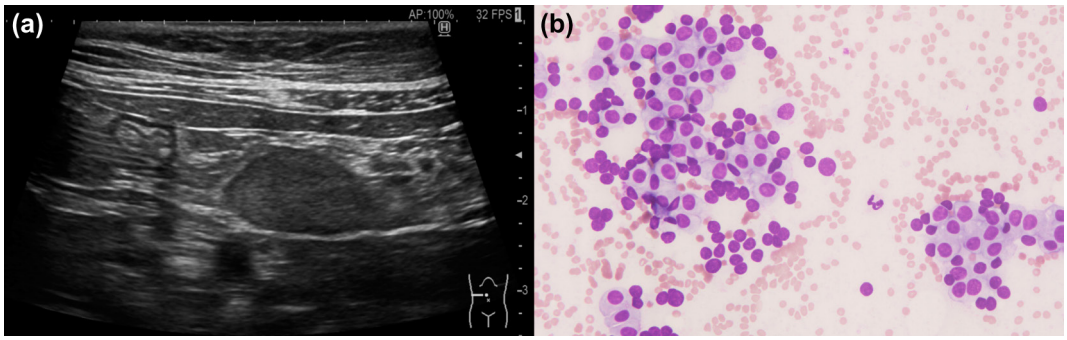

Fig. 1. (**a**) Abdominal ultrasonography revealing an oval isoechoic mass; (**b**) ultrasound-guided fine-needle aspiration revealing clusters of epithelial cells with light basophilic cytoplasm and oval nuclei containing fine reticular chromatin (Wright-Giemsa stain, ×400).

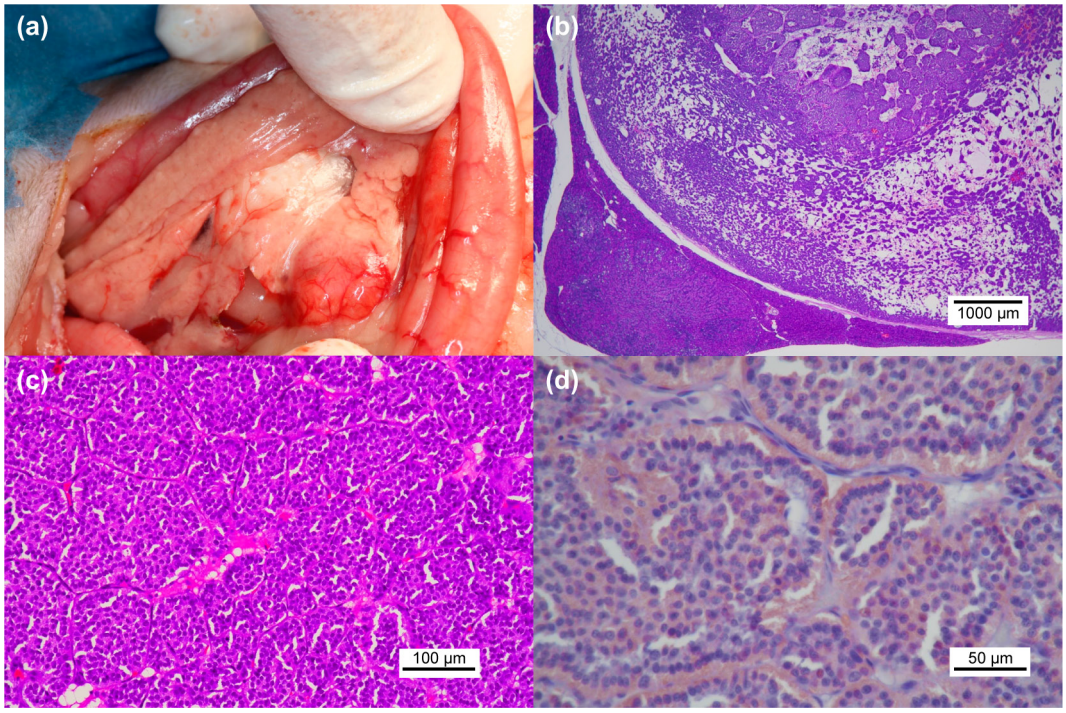

Fig. 2. The right lobe mass is histopathologically and immunohistochemically determined to be an insulinoma; (**a**) macroscopic appearance; (**b**) hematoxylin and eosin stain (×20); (**c**) hematoxylin and eosin stain (×200); (**d**) immunohistochemistry for insulin (×400).

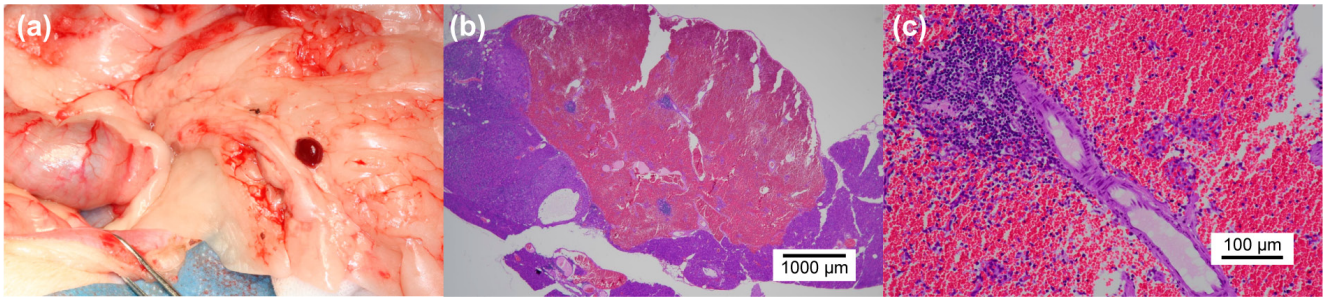

Fig. 3. The left lobe nodule is histopathologically determined to be an ectopic splenic tissue; (**a**) macroscopic appearance; (**b**) hematoxylin and eosin stain (×20); (**c**) hematoxylin and eosin stain (×200).

same level of each pancreatic lesion.

On reevaluation, during the post-contrast series, hyper-attenuation and hypo-attenuation were defined as a positive or negative difference of at least 20 HU between the mass and the normal surrounding pancreatic parenchyma or the normal splenic parenchyma. Isoattenuation was defined as attenuation within 20 HU of the normal surrounding pancreatic parenchyma or the normal splenic parenchyma [8, 9].

The lesion of insulinoma was isoattenuating to the normal surrounding pancreatic parenchyma and the normal splenic parenchyma in the pre-contrast series (37 vs. 40 vs. 53 HU, respectively). However, this lesion was hyper-attenuating to the normal surrounding pancreatic parenchyma and the normal splenic parenchyma in all post-contrast series, especially during the late arterial phase (early arterial phase, 137 vs. 87 vs. 110 HU; late arterial phase, 344 vs. 137 vs. 262 HU; portal vein phase, 271 vs. 120 vs. 230 HU; equilibrium phase, 223 vs. 114 vs. 176 HU) (Fig. 4).

The lesion of ectopic splenic tissue was isoattenuating to the normal surrounding pancreatic parenchyma but hypo-attenuating to the normal splenic parenchyma in the pre-contrast series (35 vs. 32 vs. 60 HU, respectively). In all post-contrast series, this lesion was also hyper-attenuating to the normal surrounding pancreatic parenchyma, especially during the late arterial phase (early arterial phase, 86 vs. 51 HU; late arterial phase, 239 vs. 122 HU; portal vein phase, 173 vs. 92 HU; equilibrium phase, 133 vs. 91 HU). However, in all post-contrast series except for the late arterial phase, this lesion was hypo-attenuating to the normal splenic parenchyma (early arterial phase, 86 vs. 119 HU; portal vein phase, 173 vs. 207 HU; equilibrium phase, 133 vs. 165 HU). During the late arterial phase, this lesion was isoattenuating to the normal splenic parenchyma (239 vs. 247 HU, respectively) (Fig. 5).

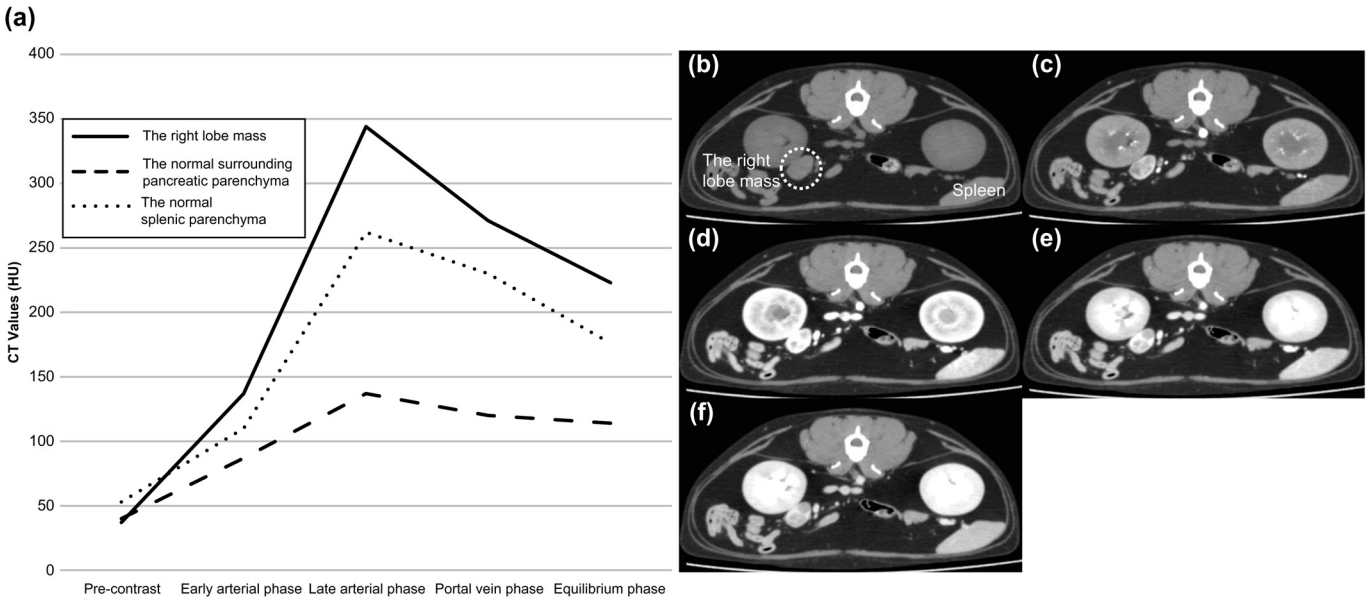

Fig. 4. Hyper-attenuation of the right lobe mass in the normal surrounding pancreatic parenchyma and in the normal splenic parenchyma in all the post-contrast series, especially during the late arterial phase; (**a**) time-attenuation curve; (**b**) pre-contrast; (**c**) early arterial phase; (**d**) late arterial phase; (**e**) portal vein phase; (**f**) equilibrium phase.

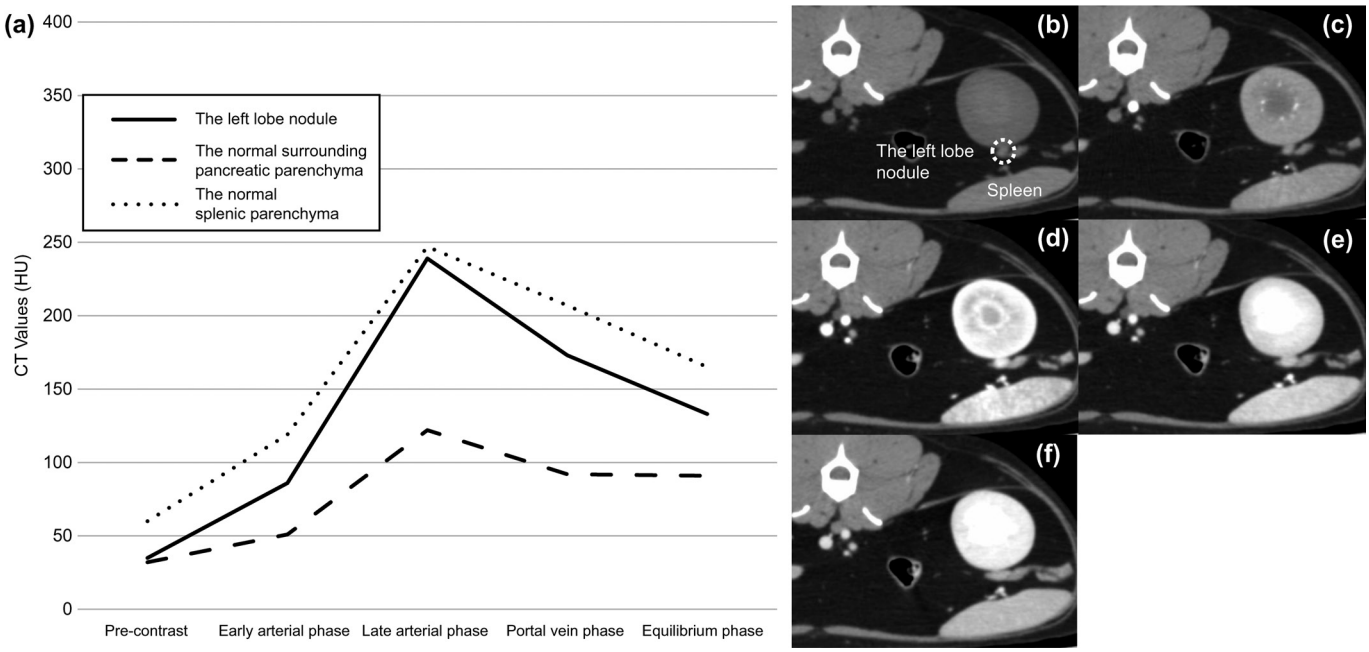

Fig. 5. Hyper-attenuation and hypo-attenuation of the left lobe nodule in the normal surrounding pancreatic parenchyma, especially during the late arterial phase, and in the normal splenic parenchyma, except for in the late arterial phase, respectively; (**a**) time-attenuation curve; (**b**) pre-contrast; (**c**) early arterial phase; (**d**) late arterial phase; (**e**) portal vein phase; (**f**) equilibrium phase.

A report of dual-phase contrast-enhanced CT findings in feline pancreatic insulinoma indicated similar hyper-attenuation during the arterial phase [34]. In this case, although the number of phases were different, the mass was hyper-attenuating most during the late arterial phase on dynamic abdominal four-phase contrast-enhanced CT, which was consistent with the previous report. A previous study on canine pancreatic insulinoma confirmed hypo-attenuation during the arterial phase [8]; however, three reports on multi-phase contrast-enhanced CT indicated that hyper-attenuation during the arterial phase was the dominant attenuation pattern [6, 14, 24]. Therefore, it is assumed that hyper-attenuation during the arterial phase is the major attenuation pattern in cats as well. Furthermore, it has been suggested that triple-phase contrast-enhanced CT provides superior preoperative imaging of canine

insulinomas [2]. Therefore, at our facility, four-phase series were obtained for every dynamic CT scan for pancreatic diseases using the modified bolus-tracking technique [5].

Sensitivity of abdominal ultrasonography for the detection of canine insulinomas is variable in less than approximately 70% of cases [8, 20, 24, 31]. Ultrasonographic echogenicity of canine insulinomas have been reported as hypoechoic [20, 24, 31]. However, that of the mass in this case was isoechoic, which was inconsistent with previous feline cases [4, 11, 33, 34]. Variations of echogenicity might also contribute to the reduced detection sensitivity of abdominal ultrasonography in feline insulinomas.

Ectopic spleen reportedly presents as a mass with CT findings similar to normal spleen in humans [19, 30]. To the best of our knowledge, this is the first report of CT findings of feline IPAS. Differentiation from splenosis was based on the location of the lesion within the left pancreatic lobe, with no other lesions from the omentum or adjacent viscera and no evidence or prior history of splenic trauma in this case [36]. The CT values of IPAS did not exceed those of normal splenic parenchyma and showed similar variability in all post-contrast series. In retrospect, these CT findings were different from those of insulinoma and have suggested that the lesion might be ectopic spleen. Furthermore, the lesion was not delineated from the left lobe parenchyma on abdominal ultrasonography, which might be one of the findings of IPAS. The lesions of IPAS were not found on abdominal ultrasonography even in previous feline cases [29].

In human medicine, IPAS can be difficult to separate from malignant neuroendocrine tumor or metastasis. Several reports have reported that SPECT and MRI were useful diagnostic imaging modalities in differentiating benign IPAS from other malignancies [15, 40]. Although there were only two dog IPAS cases mimicking metastasis of splenic hemangiosarcoma on abdominal sonography [29] in veterinary medicine, one veterinary pathological facility reported ectopic splenic tissue was seen in 24 out of 540 cases of routinely submitted feline pancreas samples [38]. IPAS might be underdiagnosed because of the lack of symptoms and the difficulty with its detection in routine clinical examination. However, distinguishing IPAS from other pancreatic malignancies on dynamic abdominal CT might be important, as such differences might influence the treatment decision.

When an intrapancreatic lesion which shows hyper-attenuation on dynamic abdominal CT is detected, not only insulinoma or metastasis of malignancies, but also IPAS should be considered as differential diagnoses. Further studies are warranted to investigate the attenuation patterns of the feline pancreatic insulinoma and IPAS on dynamic abdominal CT to avoid pitfalls in the interpretation of pancreatic imaging.

CONFLICT OF INTEREST. The authors have no conflicts of interest to declare.

ACKNOWLEDGMENTS. The authors thank the owners of the cat and all staff members of the Japan Small Animal Medical Center.

REFERENCES

1. Buchbinder, J. H. and Lipkoff, C. J. 1939. Splenosis: multiple peritoneal splenic implants following abdominal injury. *Surgery* **6**: 927–934.
2. Buishand, F. O., Vilaplana Grosso, F. R., Kirpensteijn, J. and van Nimwegen, S. A. 2018. Utility of contrast-enhanced computed tomography in the evaluation of canine insulinoma location. *Vet. Q.* **38**: 53–62. [Medline] [CrossRef]
3. Caywood, D. D., Klausner, J. S., O'Leary, T. P., Withrow, S. J., Richardson, R. C., Harvey, H., Norris, A., Henderson, R. and Johnston, S. 1988. Pancreatic insulin-secreting neoplasms: clinical, diagnostic, and prognostic features in 73 dogs. *J. Am. Anim. Hosp. Assoc.* **24**: 577–584.
4. Cervone, M., Harel, M., Ségard-Weisse, E. and Krafft, E. 2019. Use of contrast-enhanced ultrasonography for the detection of a feline insulinoma. *JFMS Open Rep* **5**: 2055116919876140. [Medline]
5. Choi, S. Y., Lee, I., Seo, J. W., Park, H. Y., Choi, H. J. and Lee, Y. W. 2016. Optimal scan delay depending on contrast material injection duration in abdominal multi-phase computed tomography of pancreas and liver in normal Beagle dogs. *J. Vet. Sci.* **17**: 555–561. [Medline] [CrossRef]
6. Coss, P., Gilman, O., Warren-Smith, C. and Major, A. C. 2021. The appearance of canine insulinoma on dual phase computed tomographic angiography. *J. Small Anim. Pract.* **62**: 540–546. [Medline] [CrossRef]
7. Fremont, R. D. and Rice, T. W. 2007. Splenosis: a review. *South. Med. J.* **100**: 589–593. [Medline] [CrossRef]
8. Fukushima, K., Fujiwara, R., Yamamoto, K., Kanemoto, H., Ohno, K., Tsuboi, M., Uchida, K., Matsuki, N., Nishimura, R. and Tsujimoto, H. 2016. Characterization of triple-phase computed tomography in dogs with pancreatic insulinoma. *J. Vet. Med. Sci.* **77**: 1549–1553. [Medline] [CrossRef]
9. Fukushima, K., Kanemoto, H., Ohno, K., Takahashi, M., Nakashima, K., Fujino, Y., Uchida, K., Fujiwara, R., Nishimura, R. and Tsujimoto, H. 2012. CT characteristics of primary hepatic mass lesions in dogs. *Vet. Radiol. Ultrasound* **53**: 252–257. [Medline]
10. Garden, O. A., Reubi, J. C., Dykes, N. L., Yeager, A. E., McDonough, S. P. and Simpson, K. W. 2005. Somatostatin receptor imaging in vivo by planar scintigraphy facilitates the diagnosis of canine insulinomas. *J. Vet. Intern. Med.* **19**: 168–176. [Medline] [CrossRef]
11. Gifford, C. H., Morris, A. P., Kenney, K. J. and Estep, J. S. 2020. Diagnosis of insulinoma in a Maine Coon cat. *JFMS Open Rep* **6**: 2055116919894782. [Medline]
12. Greene, S. N. and Bright, R. M. 2008. Insulinoma in a cat. *J. Small Anim. Pract.* **49**: 38–40. [Medline]
13. Hawks, D., Peterson, M. E., Hawkins, K. L. and Rosebury, W. S. 1992. Insulin-secreting pancreatic (islet cell) carcinoma in a cat. *J. Vet. Intern. Med.* **6**: 193–196. [Medline] [CrossRef]
14. Iseri, T., Yamada, K., Chijiwa, K., Nishimura, R., Matsunaga, S., Fujiwara, R. and Sasaki, N. 2007. Dynamic computed tomography of the pancreas in normal dogs and in a dog with pancreatic insulinoma. *Vet. Radiol. Ultrasound* **48**: 328–331. [Medline] [CrossRef]
15. Kang, B. K., Kim, J. H., Byun, J. H., Lee, S. S., Kim, H. J., Kim, S. Y. and Lee, M. G. 2014. Diffusion-weighted MRI: usefulness for differentiating intrapancreatic accessory spleen and small hypervascular neuroendocrine tumor of the pancreas. *Acta Radiol.* **55**: 1157–1165. [Medline] [CrossRef]
16. Kraje, A. C. 2003. Hypoglycemia and irreversible neurologic complications in a cat with insulinoma. *J. Am. Vet. Med. Assoc.* **223**: 812–814, 810. [Medline] [CrossRef]
17. Kruth, S. A., Feldman, E. C. and Kennedy, P. C. 1982. Insulin-secreting islet cell tumors: establishing a diagnosis and the clinical course for 25 dogs. *J. Am. Vet. Med. Assoc.* **181**: 54–58. [Medline]
18. Ksiadzyna, D. and Peña, A. S. 2011. Abdominal splenosis. *Rev. Esp. Enferm. Dig.* **103**: 421–426. [Medline]

19. Lake, S. T., Johnson, P. T., Kawamoto, S., Hruban, R. H. and Fishman, E. K. 2012. CT of splenosis: patterns and pitfalls. *AJR Am. J. Roentgenol.* **199**: W686-93. [Medline] [CrossRef]
20. Lamb, C. R., Simpson, K. W., Boswood, A. and Matthewman, L. A. 1995. Ultrasonography of pancreatic neoplasia in the dog: a retrospective review of 16 cases. *Vet. Rec.* **137**: 65–68. [Medline] [CrossRef]
21. Leifer, C. E., Peterson, M. E. and Matus, R. E. 1986. Insulin-secreting tumor: diagnosis and medical and surgical management in 55 dogs. *J. Am. Vet. Med. Assoc.* **188**: 60–64. [Medline]
22. Lester, N. V., Newell, S. M., Hill, R. C. and Lanz, O. I. 1999. Scintigraphic diagnosis of insulinoma in a dog. *Vet. Radiol. Ultrasound* **40**: 174–178. [Medline] [CrossRef]
23. Madarame, H., Kayanuma, H., Shida, T. and Tsuchiya, R. 2009. Retrospective study of canine insulinomas: eight cases (2005–2008). *J. Vet. Med. Sci.* **71**: 905–911. [Medline] [CrossRef]
24. Mai, W. and Cáceres, A. V. 2008. Dual-phase computed tomographic angiography in three dogs with pancreatic insulinoma. *Vet. Radiol. Ultrasound* **49**: 141–148. [Medline] [CrossRef]
25. McMillan, F. D., Barr, B. and Feldman, E. C. 1985. Functional pancreatic islet cell tumor in a cat. *J. Am. Anim. Hosp. Assoc.* **21**: 741–746.
26. Nakamura, K., Lim, S. Y., Ochiai, K., Yamasaki, M., Ohta, H., Morishita, K., Takagi, S. and Takiguchi, M. 2015. Contrast-enhanced ultrasonographic findings in three dogs with pancreatic insulinoma. *Vet. Radiol. Ultrasound* **56**: 55–62. [Medline] [CrossRef]
27. O'Brien, T. D., Norton, F., Turner, T. M. and Johnson, K. H. 1990. Pancreatic endocrine tumor in a cat: clinical, pathological, and immunohistochemical evaluation. *J. Am. Anim. Hosp. Assoc.* **26**: 453–457.
28. Polton, G. A., White, R. N., Brearley, M. J. and Eastwood, J. M. 2007. Improved survival in a retrospective cohort of 28 dogs with insulinoma. *J. Small Anim. Pract.* **48**: 151–156. [Medline] [CrossRef]
29. Ramírez, G. A., Altimira, J., García-González, B. and Vilafranca, M. 2013. Intrapancreatic ectopic splenic tissue in dogs and cats. *J. Comp. Pathol.* **148**: 361–364. [Medline] [CrossRef]
30. Rashid, S. A. 2014. Accessory spleen: prevalence and multidetector CT appearance. *Malays. J. Med. Sci.* **21**: 18–23. [Medline]
31. Robben, J. H., Pollak, Y. W. E. A., Kirpensteijn, J., Boroffka, S. A. E. B., van den Ingh, T. S. G. A. M., Teske, E. and Voorhout, G. 2005. Comparison of ultrasonography, computed tomography, and single-photon emission computed tomography for the detection and localization of canine insulinoma. *J. Vet. Intern. Med.* **19**: 15–22. [Medline] [CrossRef]
32. Robben, J. H., Visser-Wisselaar, H. A., Rutteman, G. R., van Rijk, P. P., van Dongen, A. J., Voorhout, G., van den Ingh, T. S., Hofland, L. J. and Lamberts, S. W. 1997. In vitro and in vivo detection of functional somatostatin receptors in canine insulinomas. *J. Nucl. Med.* **38**: 1036–1042. [Medline]
33. Schaub, S. and Wigger, A. 2013. Ultrasound-aided diagnosis of an insulinoma in a cat. *Tierarztl. Prax. Ausg. K Klientiere. Heimtiere* **41**: 338–342. [Medline] [CrossRef]
34. Shorten, E., Swallow, A., McCallum, K. E., Holzhausen, C., Hughes, K. and Genain, M. A. 2020. Computed tomographic findings in a case of feline insulinoma. *Vet. Rec. Case Rep.* **8**: e001054. [CrossRef]
35. Spangler, W. L. and Culbertson, M. R. 1992. Prevalence and type of splenic diseases in cats: 455 cases (1985–1991). *J. Am. Vet. Med. Assoc.* **201**: 773–776. [Medline]
36. Tabaran, F., Catoi, C., Ardelean, A. S., Gal, F. A. and O'Sullivan, G. 2019. Intrapancreatic heterotopic splenic tissue in cats: An overlooked diagnosis? *J. Comp. Pathol.* **166**: 135. [CrossRef]
37. Tobin, R. L., Nelson, R. W., Lucroy, M. D., Wooldridge, J. D. and Feldman, E. C. 1999. Outcome of surgical versus medical treatment of dogs with beta cell neoplasia: 39 cases (1990–1997). *J. Am. Vet. Med. Assoc.* **215**: 226–230. [Medline]
38. Törner, K., Staudacher, M., Steiger, K. and Aupperle-Lellbach, H. 2020. Clinical and pathological data of 17 non-epithelial pancreatic tumors in cats. *Vet. Sci.* **7**: 55. [Medline] [CrossRef]
39. Vanderperren, K., Haers, H., Van der Vekens, E., Stock, E., Paepe, D., Daminet, S. and Saunders, J. H. 2014. Description of the use of contrast-enhanced ultrasonography in four dogs with pancreatic tumours. *J. Small Anim. Pract.* **55**: 164–169. [Medline] [CrossRef]
40. Zurek Munk-Madsen, M., Zakarian, K., Sandor Oturai, P., Hansen, C. P., Federspiel, B., Fallentin, E. and Linno Willemoe, G. 2019. Intrapancreatic accessory spleen mimicking malignant tumor: three case reports. *Acta Radiol. Open* **8**: 2058460119859347. [Medline]